Wear 330-331 (2015) 103–111

Contents lists available at ScienceDirect

Wear

journal homepage: www.elsevier.com/locate/wear

The role of frictional power dissipation (as a function of frequency) and test temperature on contact temperature and the subsequent wear behaviour in a stainless steel contact in fretting

X. Jin *, P.H. Shipway, W. Sun

Division of Materials, Mechanics and Structures, Faculty of Engineering, University of Nottingham, Nottingham, UK

ARTICLE INFO

Article history:
Received 3 September 2014
Received in revised form
21 January 2015
Accepted 6 February 2015

Keywords:
Fretting wear
Contact temperature
Stainless steel
Frequency
Debris

ABSTRACT

Temperature is known to affect the fretting wear behaviour of metals; generally, a critical temperature is observed, above which there are substantial reductions in wear rate, with these being associated with the development of protective oxide beds in the fretting contact. This work has examined the gross-sliding fretting behaviour of a stainless steel as a function of bulk temperature and fretting frequency (with changes in the fretting frequency altering the frictional power dissipated in the contact amongst other things). An analytical model has been developed which has suggested that at 200 Hz, an increase in the contact temperature of more than 70 °C can be expected, associated with the high frictional power dissipation at this frequency (compared to that dissipated at a fretting frequency of 20 Hz). With the bulk temperature at either room temperature or 275 °C, the increase in contact temperature does not result in a transition across the critical temperature (and thus fretting behaviour at these temperatures is relatively insensitive to fretting frequency). However, with a bulk temperature of 150 °C, the increase in temperature associated with the increased frictional power dissipation at the higher frequency results in the critical temperature being exceeded, and in significant differences in fretting behaviour.

1. Introduction

Fretting is the small amplitude oscillation between two bodies in contact which occurs in a wide variety of mechanical systems. Although the amplitude of fretting is small ($<300\ \mu m$), fretting can cause serious damage including wear and fatigue. It has been stated that over 50 parameters can influence behaviour in fretting [1]; amongst them, the temperature of the contact has been identified as having a significant influence on both the rate and mechanism of damage in fretting. The role of temperature in fretting has generally been attributed to changes in the rate of formation of oxide in the fretting contact, and to changes in the way that the oxide debris is either expelled from the contact or retained within the contact.

Previous studies have suggested that the fretting wear rate of both carbon and stainless steel tends to fall rapidly once a certain critical ambient test temperature has been exceeded [2–5]. However, the fretting process itself also influences the contact temperature due to the dissipation of frictional power through the contact. This is dependent on the applied load, the coefficient of friction, the slip amplitude and the frequency of oscillation (with this paper focussing on the role of fretting frequency in this regard). As the fretting frequency increases, the temperature within the contact will also increase, and it is argued that this will affect the debris formation and debris retention within the contact by mechanisms similar to those proposed when the role of ambient temperature has been considered. Indeed, a general reduction of wear rate has been found with increasing fretting frequency in previous studies [6–8]. Frequency was chosen as the main controlling parameter as (all other things being equal) the frictional power dissipation is simply proportional to fretting frequency; this is in contrast to changes in load (which will affect the tractional force required for sliding of the contact, and will thus change the slip amplitude as well as the frictional force) and changes in displacement amplitude (which will affect the frictional power dissipation but will also affect the area over which that frictional power is dissipated); accordingly, variations in the frequency provide the simplest route to understanding the role of dissipated frictional power density on the temperature and subsequent fretting behaviour of such a contact.

As already identified, wear behaviour in fretting depends critically on the creation of oxide debris and the retention/ejection of that debris from the contact. It has been demonstrated by a number of workers (e.g. Colombie et al. [9], Iwabuchi et al. [5]) that the rate and mechanism of wear is very sensitive to the formation of a stable oxide debris layer. It was argued that a stable

* Corresponding author.
E-mail address: eaxxj@exmail.nottingham.ac.uk (X. Jin).

http://dx.doi.org/10.1016/j.wear.2015.02.022

debris bed acts as a third body between the two contacting parts in that it separates the wear surfaces and functions as a solid bearing to protect the primary surfaces [10]. However, if a stable debris layer cannot be formed, the existence of the oxide particles may increase the wear rate as they act in an abrasive manner. It has been proposed by Jiang et al. [11] that it is the inter-particle adhesion force that affects the formation of a stable layer. With a stronger inter-particle adhesion force, the oxide particles are more readily formed into a stable debris layer rather than being expelled from the contact. It is suggested that with increasing temperature, the surface free energy of the oxide particles increases, and that this will increase the adhesive force between the particles and encourage the formation of a stable debris layer [11].

Whilst sintering of particulate materials is generally only significant at temperatures above approximately a half of the melting point of the material [12], it has been demonstrated that sintering can occur at much lower temperatures, either with very fine particles [13,14] or under tribologically-active conditions [13–15]. By supplying fine iron oxide particles into a sliding interface, sintering has been demonstrated at room temperature by Kato [14] and Kato and Komai [13]. In addition, the study of Pearson et al. [16] on a high strength steel argued that debris sintering occurred at temperatures as low as 85 °C in fretting.

The effect of frequency on fretting behaviour has often been attributed to its effect on the kinetics of formation of oxide debris. Uhlig and co-workers [6,7] observed that the wear rate in a steel contact fell by about 58% with increasing fretting frequency from around 1 Hz to 50 Hz; moreover, the effects of the frequency were greater with larger displacement amplitudes (and thus larger frictional power dissipation in the contact). In addition, Feng and Uhlig [7] also demonstrated that the effect of frequency disappeared when the tests were conducted in an inert (nitrogen) atmosphere, clearly indicating that the frequency effects were intrinsically linked to oxide formation. In fretting, asperities in the contact interact, resulting in the exposure of clean metallic surfaces; the oxidation of that nascent metal is both a temperature-dependent and time-dependent process. High fretting frequencies can encourage the formation of oxides by raising the contact temperature; however, at the same time, an increase in fretting frequency reduces the time for oxidation between interactions of the asperities in the contact. The amplification of any effects of fretting frequency with displacement amplitude [17–19] is associated with the increase in frictional power dissipation (recognising that there are also changes in the area over which the power is dissipated associated with changes in displacement amplitude, but typically only for one of the bodies in the contact in a non-conforming contact).

It can be seen that both environmental bulk temperature and the fretting frequency have a critical influence on behaviour in fretting, and it is argued that these two influences are not entirely independent. The study of contact temperature associated with dissipation of frictional power in a contact has a long history, with its significance in wear being well-recognised. Blok identified the role of what was termed the “flash temperature” [20], and since that time, many mathematical models have been created to calculate the temperature rise associated with frictional power dissipation in both sliding and fretting contacts [21–25]. In the current work, both fretting frequency and environmental temperature were varied in order to explore the various influences on the contact temperature and the subsequent wear within a stainless steel contact. The effects of these two influences upon the magnitude and mechanisms of damage were explored, facilitating an understanding of the dominant influences.

Table 1
Chemical composition of 304 stainless steel (wt%).

C	Si	Mn	P	S	Cr	Mo	Ni
0.027	0.816	1.79	0.013	0.025	17.2	0.303	10.3
Al	Co	Cu	Nb	Ti	V	W	Fe
0.003	0.083	0.347	0.012	0.008	0.044	0.035	Remainder

2. Experimental procedure

2.1. Specimen, test procedures and conditions

Fretting experiments were conducted on 304 stainless steel specimens; the chemical composition of this steel is detailed in Table 1. Specimens were assembled in a cylinder-on-flat arrangement (Fig. 1) which generated a line contact with a length of 10 mm. The flat specimen was mounted on the lower specimen mounting block (LSMB) which is stationary and the cylindrical specimen was mounted on the upper specimen mounting block (USMB). A normal load, P, was applied to the USMB through a dead-weight. The fretting motion was applied perpendicular to the axis of the cylindrical specimen through control of an electromagnetic vibrator (EMV). The far-field displacement of the USMB was measured through a capacitance displacement sensor which facilitated control of the relative displacement between the specimens. The EMV was guided axially by leaf springs to apply a displacement to the USMB as shown in Fig. 2. A piezoelectric load cell was used to measure the tangential force in the contact. The displacement and the tangential force were recorded continuously (200 samples per fretting cycle) and were plotted against each other as fretting loops. The maximum reaction force (Q*) in each cycle was recorded. A schematic fretting loop (representative of those observed during the tests conducted) is presented in Fig. 3, along with an example of a measured fretting loop. The slip amplitude (δ) represents the actual slip that occurs in the contact; it is measured from the fretting loops and is usually smaller than the applied displacement amplitude (Δ) due to compliances in the contact and in the system more generally. The energy coefficient of friction (ECoF), calculated from the dissipated energy per cycle (E_d), was employed in this study as follows:

$$\mathrm{ECoF} = \frac{E_d}{4\,P\,\delta}$$

The stiffness of the system, S, is defined as the gradient of the steep side of the fretting loop (see Fig. 3a), which corresponds to measured displacements under conditions when the contact is not sliding [26,27]. Fig. 3b shows an example of an experimentally-measured fretting loop; from loops such as this, the system stiffness, S, can be estimated to lie in the range of 30–37 MN m^{-1}.

Cartridge heaters were integrated into the LSMB and a plate heater was assembled above the cylindrical specimen on the USMB to allow control of the temperature of each specimen. Open wire thermocouples were welded onto the top surface of each of

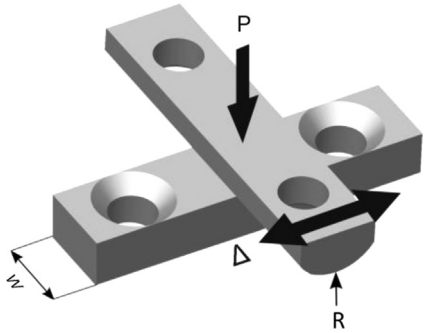

Fig. 1. Cylinder-on-flat specimen arrangement in fretting test: W=10 mm, R=6 mm, P=450 N, and Δ=50 μm [8].

the specimens and the temperatures recorded were used in individual control loops for each specimen; in this work, both specimens were maintained at the same temperature.

Tests were performed with temperatures from ambient to 275 °C with both a low frequency (20 Hz) and a high frequency (200 Hz) of fretting. Test conditions are summarised in Table 2.

2.2. Estimation of wear volume and wear rate

After the completion of a fretting experiment, the specimens were lightly swabbed with industrial methylated spirit to remove loose debris, thus leaving any debris that was adhered to the specimen in place. The wear scars on both the flat and cylindrical specimens were scanned with a Bruker contour GT-I interferometer to evaluate their topography. The system has a vertical resolution of ~0.15 nm and a lateral resolution of 4 μm. The scan area on the flat specimen was 5 mm in width and 10.5 mm in length; scans on the cylinders were 3 mm in width and 13 mm in length. The profiles of the surface outside the wear scar were used to create a reference surface (representation the surface profile of the whole surface before wear occurred). The volume below each reference surface was regarded as the wear volume (V^-_{Flat} and V^-_{Cyl} for the flat and cylindrical specimens, respectively) and the volume of material above these surfaces was regarded as transferred volume (V^+_{Flat} and V^+_{Cyl} for the flat and cylindrical specimens, respectively). The total wear and transfer volumes for the couple (V^- and V^+, respectively) are defined as the sum of the respective volumes for the flat and cylindrical specimens. Wear and transfer rates for the contact pair were calculated based on the slip amplitude (δ) and the number of cycles per test (N), as indicated in Eqs. (1) and (2). The net wear rate (NWR) indicates the total material loss which is defined as the difference between the wear and transfer rates, as shown in Eq. (3).

$$\text{Wear rate}: \dot{V}^- = \frac{V^-}{4\,\delta\,P\,N} \tag{1}$$

$$\text{Transfer rate}: \dot{V}^+ = \frac{V^+}{4\,\delta\,P\,N} \tag{2}$$

$$\text{Net wear rate}: \text{NWR} = \dot{V}^- - \dot{V}^+ \tag{3}$$

Scanning electron microscopy (SEM) was used to image the wear scars using back-scattered electron (BSE) imaging. The BSE images were used to identify the distribution of oxide debris within the wear scars, since the oxides exhibit a lower brightness than the steel in this imaging mode.

2.3. Temperature measurements associated with the fretting of the contact

A separate test was performed to identify the local temperature rise due to frictional power dissipation in the contact. The test was performed under similar conditions as the full wear tests (P=450 N, Δ=50 μm), but with the test only being run at a frequency of 200 Hz for 1000 s. The temperatures close to the contact were measured via fine, sheathed thermocouples. As shown in Fig. 4, holes of 0.3 mm diameter were drilled in the flat specimen, with the axis of the hole parallel to that of the line contact. The holes were drilled directly below the position of the fretting line contact at depths of 0.45 mm, 1.05 mm and 2.5 mm below the surface. Each hole was 5 mm in depth such that when thermocouples were inserted, the thermocouple tip was central along the 10 mm contact line. Sheathed thermocouples of 0.25 mm diameter were inserted into the holes. As the drilling of the hole removed part of the specimen material, it was recognised that its presence may influence the temperature distribution

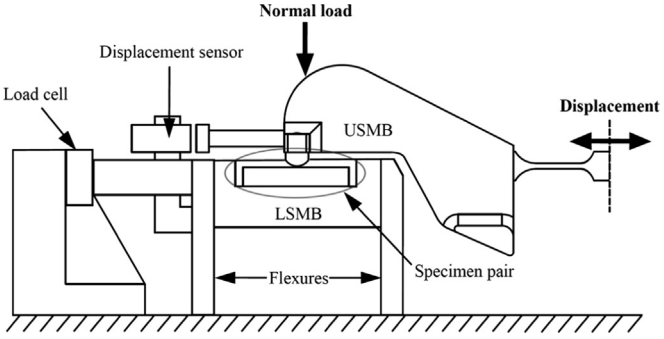

Fig. 2. Main components of fretting apparatus [8].

Table 2
Fretting test conditions.

Normal load	P (N)	450
Applied displacement	Δ (μm)	50
Duration	N (cycles)	100,000
Frequency	f (Hz)	20, 200
Temperature	T (°C)	Amb, 150, 275

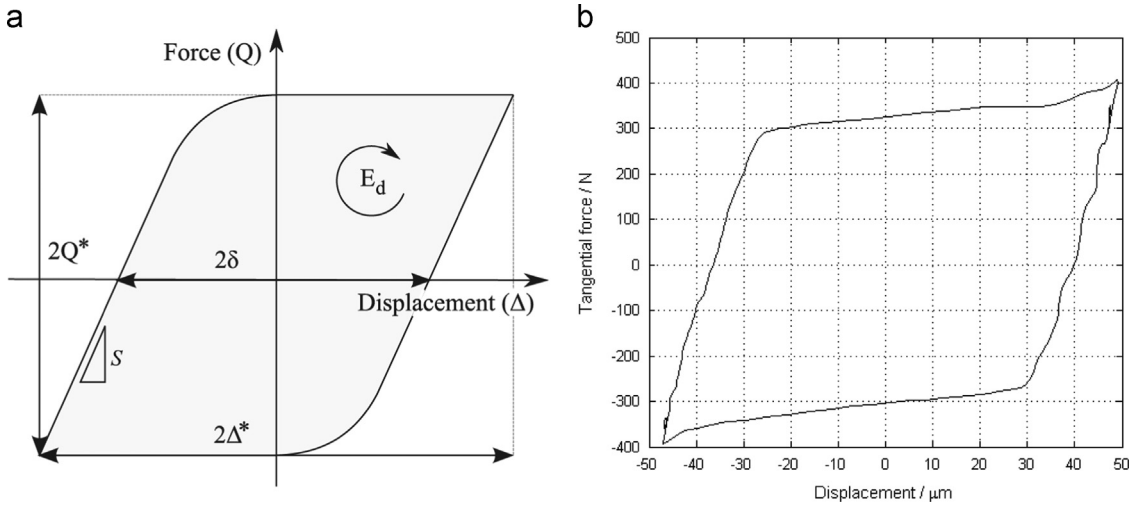

Fig. 3. (a) Schematic fretting loop [16]. (b) Experimental fretting loop (90,000 cycles, P=450 N, f=20 Hz, Δ=50 μm, room temperature).

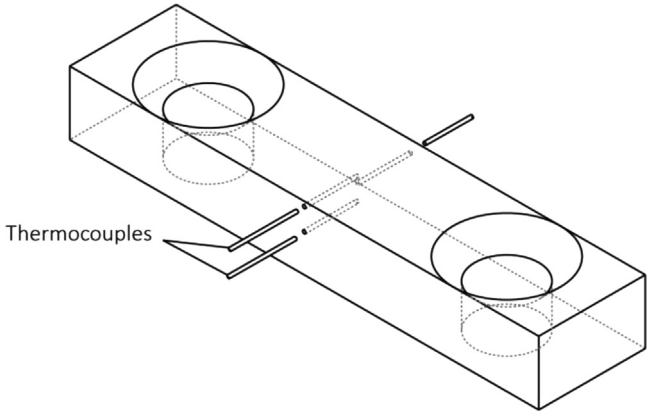

Fig. 4. Illustration of the positions of the thermocouples.

around the holes. To minimise this influence, the holes 0.45 mm and 2.5 mm from the surface were drilled from one side of the specimen while the hole 1.05 mm from the surface was drilled from the other side of the specimen.

3. Simplified mathematical model of the temperature field in a fretting contact

A mathematical model has been developed to predict the temperature rise in the contact based upon the frictional power dissipation. There are complexities in the calculation of the frictional temperature rise in a moving contact; however, under fretting conditions, the slider performs a reciprocating motion with displacement amplitudes which are small. Therefore, the variation in the position of heat source can be reasonably neglected. Greenwood and Alliston-Greiner [24] assumed a static heat source with a sinusoidal heat flow to represent a fretting heat input. The results have shown that the variation of the temperature due to the variations in position and power of the heat source was small. In the current work, the initial (Hertzian) half-width of the line contact is calculated to be ~57 μm (b in Eq. (6)); therefore, the slip displacement, δ, of typically 40 μm (see Fig. 3b) is relatively small in comparison with the initial contact size, and this will become a smaller fraction as the contact width increases throughout the test due to wear. Accordingly, when predicting the overall local temperature rise, the assumption is that a constant steady heat input (power) can be applied as follows:

$$q = E_d f = P\, 4\delta\, \mathrm{ECoF}\, f \tag{4}$$

where f is the frequency of fretting. The cylinder-on-flat arrangement will produce a uniform line contact, and conduction is considered to be the major form of heat dissipation in the problem. The problem can be simplified as a line heat source on a semi-infinite body, and thus treated as a 2-dimensional problem; in doing so, the role of the oxide debris bed which forms in a fretting contact is neglected in terms of the heat flows (and thus contact temperatures) in order to derive a simple analytical model. The validity of this simplification will be assessed by comparing the experimental results with those derived from the model itself.

Initially, the contact will deform elastically under load, and thus the heat will be dissipated over the area of the contact rather than over a line. The energy coefficient of friction (ECoF) is assumed to be constant across the contact (i.e. independent of contact pressure), and therefore, the power density is proportional to the contact pressure across the contact area. The contact pressure ($p(x)$) distribution for a cylinder-on-flat contact can be calculated according to the Hertz elastic contact model as follows [28]:

$$p(x) = p_0 \sqrt{1 - \frac{x^2}{b^2}} \tag{5}$$

where p_0 is the maximum contact pressure which appears at the centre of the contact area and b is the half-width of the contact. In turn, expressions for these parameters are as follows:

$$p_0 = \left(\frac{P' E}{\pi R}\right)^{1/2}, \quad b = \left(\frac{4 P' R}{\pi E}\right)^{1/2} \tag{6}$$

where P' is the normal load per unit length applied across the contact, E^* is the composite modulus of the two contacting bodies (for a cylinder-on-flat contact, R is the radius of the cylinder itself). Under plane strain conditions:

$$E^* = \left(\frac{1-(\nu_f)^2}{E_f} - \frac{1-(\nu_c)^2}{E_c}\right)^{-1} \tag{7}$$

where E_f and E_c are Young's moduli of the flat and cylindrical specimens respectively, and ν_f and ν_c are their Poisson's ratios.

Therefore, the heat input per unit time per unit area (q') (termed the power density) can be expressed as follows:

$$q'(x) = p(x)\, 4\delta\, \mathrm{ECoF}\, f \tag{8}$$

According to the solution of the temperature rise (δT) of a continuous line source on a semi-infinite space given by Carslaw and Jaeger [29]

$$\delta T = \frac{q'}{4\pi k}\left(\ln \frac{4 k t}{r^2 \rho C} - \gamma\right) \tag{9}$$

where k is the thermal conductivity, t is the time, r is the distance from the line source, ρ is the density, C is the specific heat and $\gamma = 0.5772\ldots$ is the Euler constant, the temperature rise (ΔT) at a point (x', y') in the semi-infinite body can be calculated as follows:

$$\Delta T(x', y') = \int_{-b}^{b} \delta T\, dx$$

$$\Delta T(x', y') = \int_{-b}^{b} \frac{p(x)\, 4\delta\, \mathrm{ECoF}\, f}{4\pi k}\left[\ln \frac{4kt}{\left[(x-x')^2 + y'^2\right] \rho C} - \gamma\right] dx \tag{10}$$

The initial assumption is that frictional power dissipation is the only source of heat associated with the fretting process; however, it is recognised that the formation of oxide from the metal will also contribute due to its heat of formation, and thus the validity of neglecting this contribution to the thermal balance of the system needs to be assessed. It is assumed that all of the steel worn is converted to Fe_2O_3 with a standard heat of formation of -826 kJ mol^{-1} [30] (and that the molar mass of the steel can be assumed to be the same as that of iron); the largest wear volume observed in the test programme was ~0.41 mm^3 which leads to a heat of formation of oxide in this case of ~25 J. When this is compared to the frictional energy dissipated over the same test (the sum of E_d over the test duration for the test conducted at room temperature and at 20 Hz fretting frequency) of around 5000 J, the assumption to ignore the heat of formation of the oxide is justified by it being less than 0.5% of the total heat dissipated.

4. Experimental results

4.1. Characterisation of surface damage

The total net wear rate (NWR) as a function of temperature for the two fretting frequencies is shown in Fig. 5. The dependence of the wear rates and transfer rates on temperature for the two fretting frequencies are shown in Fig. 6. It can be seen that the total material

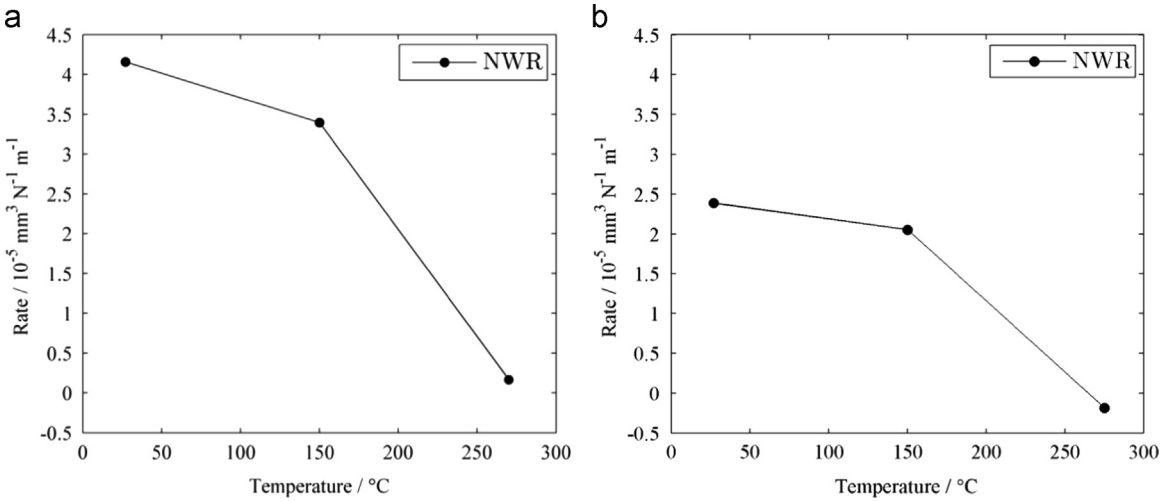

Fig. 5. Plot of net wear rate ($\dot{V}^- - \dot{V}^+$) as a function of test temperature at fretting frequencies of (a) 20 Hz and (b) 200 Hz.

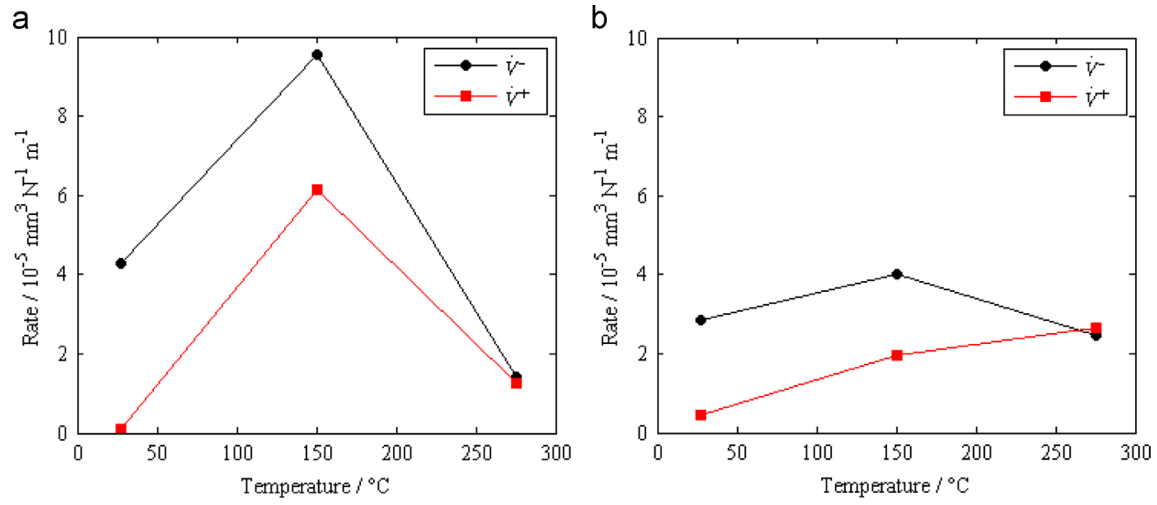

Fig. 6. Plot of wear rate ($\dot{V}^-$) and transfer rate ($\dot{V}^+$) as a function of test temperature at fretting frequencies of (a) 20 Hz and (b) 200 Hz.

loss is both temperature and frequency dependent. At both frequencies, the net wear rate decreased with the increase of temperature. A significant decrease in wear rate was observed at both frequencies at temperatures between 150 °C and 275 °C, which is in accord with the literature regarding fretting of stainless steel at elevated temperatures [4,5]. At room temperature and 150 °C, the net wear rate associated with high frequency tests are close to half of those associated with the tests conducted at the lower frequency. However, at 275 °C, the net wear rate was close to zero at both frequencies. In Fig. 6, the wear and transfer rates are plotted separately. It can be seen that at room temperature, there was almost no material transfer with the damage being primarily wear at both frequencies. However, at 150 °C, although the net wear rate dropped, $\dot{V}^-$ actually increased at both frequencies, with the increase being more significant at the lower test frequency of 20 Hz. However, $\dot{V}^+$ increased at the same time in both cases, indicating that there was significant damage in terms of material being moved around the contact. At the lower fretting frequency, $\dot{V}^-$ doubled with the increase in temperature to 150 °C with $\dot{V}^+$ increasing from almost zero to about 6×10^{-5} mm^3 N^{-1} m^{-1}. At the higher test frequency, upon increasing the temperature to 150 °C, both rates increased from their values at room temperature, but these increases were much smaller in magnitude. When the temperature was raised to 275 °C, the values of $\dot{V}^+$ and $\dot{V}^-$ became almost identical to each other at both frequencies; for the test conducted at the lower frequency, the rates were both much lower than the equivalent rates at 150 °C, but at the higher fretting frequency, no large changes in behaviour were observed.

Fig. 7 shows average profiles across the wear scars on the flat specimens for different test temperatures following testing at fretting frequencies of both 20 Hz and 200 Hz. The profiles of the cylinders are not shown as the wear behaviour has been observed to be similar on the cylinder and flat specimens for like-on-like contacts of this type [31]. The profiles were averaged along the axis of the scar so that the main features of the surface damage could be identified. At the low frequency, the scar following testing at room temperature exhibited material removal; as the temperature was raised to 150 °C, the scar became deeper, but with significant build-up of material on each side of this central wear zone. On further increasing the temperature to 275 °C, the central wear zone reduced in magnitude, as did the build-up of material to the sides of this. The behaviour at the higher test frequency showed both similarities and differences; at room temperature, the scar was predominantly wear again, with little build-up of material outside the central zone. As the temperature was raised to 150 °C, the central wear scar increased in size (to very similar dimensions to that observed following testing at the lower frequency); however, there was a notable reduction in the magnitude of the material built-up to the sides of the central wear scar when compared to the lower frequency testing. As the temperature was raised further to 275 °C, the wear scar decreased in magnitude with more material being observed in the built-up zone to each side of the central scar.

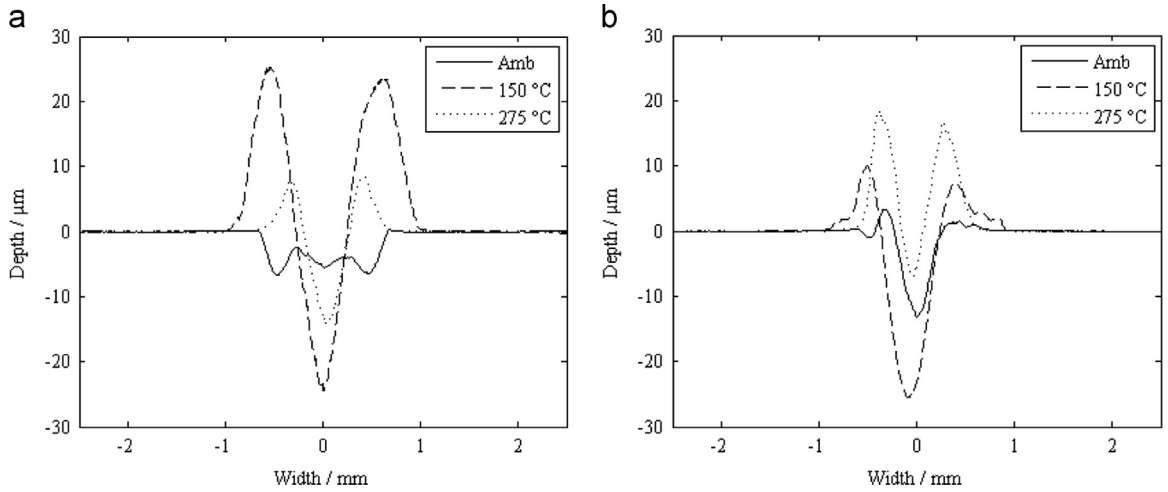

Fig. 7. Average surface profiles across the wear scars on the flat specimens as a function of test temperature for tests conducted at fretting frequencies of (a) 20 Hz and (b) 200 Hz.

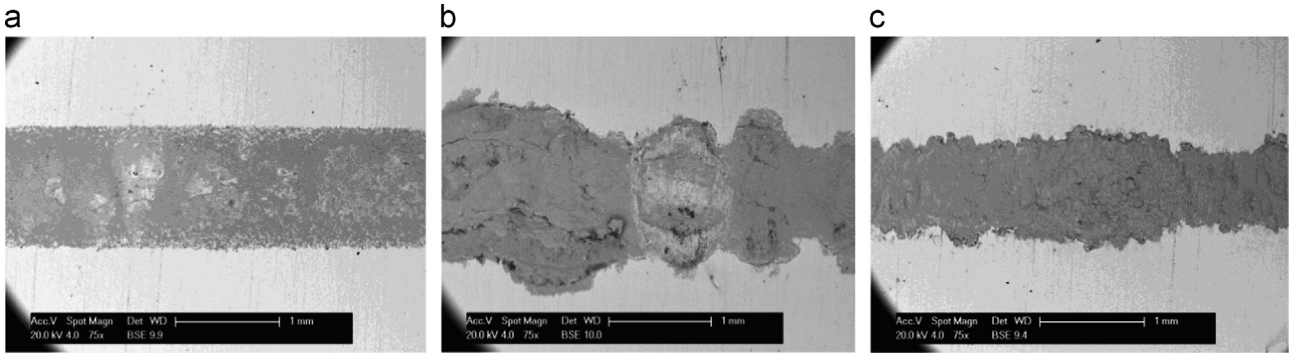

Fig. 8. (a–c) Back-scattered electron SEM plan-view micrographs of wear scars on the flat specimens following testing at 20 Hz.

Figs. 8 and 9 show BSE plan-view images of the wear scars for each test temperature following testing at 20 Hz and 200 Hz respectively. At ambient temperature, the scars from tests at both frequencies exhibited well-defined edges and relatively uniform coverage of oxide within the scar. At both frequencies, regions of the scar can be observed which show no oxide covering (brighter patches, representing a metallic surface); this indicates that oxide is being lost from the contact in both cases. There is no clear difference in the degree of oxide coverage in the wear scar as a function of frequency at ambient temperature.

At the higher test temperatures, all the scars images exhibit undulation in the edge of the wear scar, with the scar following testing at 20 Hz and 150 °C exhibiting the greatest undulation. Patches of the scars at this intermediate temperature show a much more metallic character, again indicating that oxide is being lost from the wear scars. In contrast, at the highest temperature of 275 °C, there is no evidence of any metallic character to the surface within the wear scar, indicating that the oxide is being efficiently retained in the scar at this temperature at both fretting frequencies.

4.2. Coefficient of friction

The development of the energy coefficients of friction (ECoF) throughout the fretting tests have been plotted for tests at all frequencies and temperatures (Fig. 10). It can be seen that at both frequencies, the tests conducted at 150 °C resulted in the highest ECoFs while the highest temperature (275 °C) tests resulted in the lowest steady-state ECoFs.

4.3. Local temperature

Fig. 11 shows the comparison of measured temperature rise at the contact centre and the corresponding results from the analytical model for the temperature evolution at three depths below the contact surface for fretting with a frequency of 200 Hz at ambient temperature. It can be seen that in general, the measured and predicted results correlate reasonably well for all three positions, despite experimental fluctuations being observed from all three measurement positions. As discussed previously, the model assumed an isotropic material which had constant thermal properties throughout the test duration and the heat source was based upon on the initial contact conditions. In reality, the thermal conditions may change during the fretting process especially in the region in the contact where significant changes occur (associated with changes in contact geometry and material type due to wear). However, it has been shown that despite these simplifications, the mathematical model is able to predict the overall temperature rise quite well in general.

Based on the ECoFs, the mathematical model was applied to predict the local temperature on the surface near the contact (Fig. 12). It can be seen that under the same test temperatures, the tests with higher fretting frequencies gave higher local surface temperatures. Specifically, high temperatures were predicted to occur at the centre of the contacts.

5. Discussion

It is clear that both bulk temperatures and fretting frequency have an influence on the fretting wear behaviour of 304 stainless

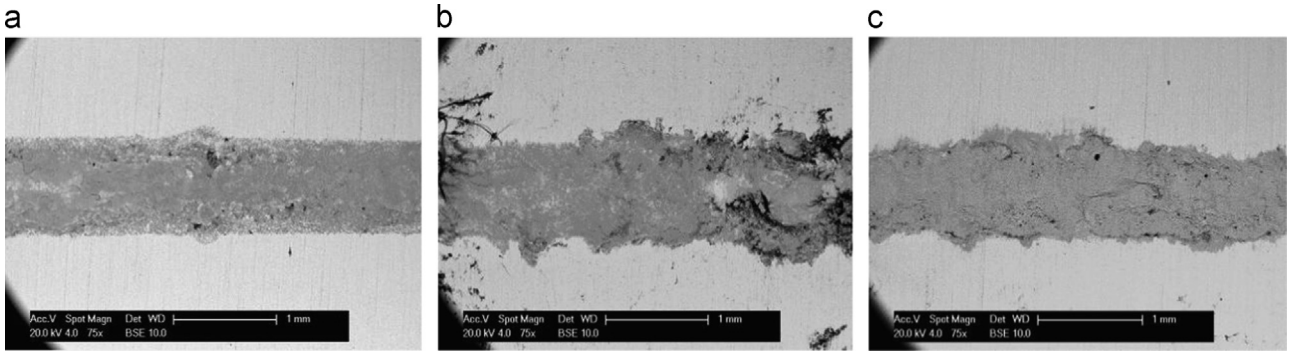

Fig. 9. (a–c) Back-scattered electron SEM plan-view micrographs of wear scars on the flat specimens following testing at 200 Hz.

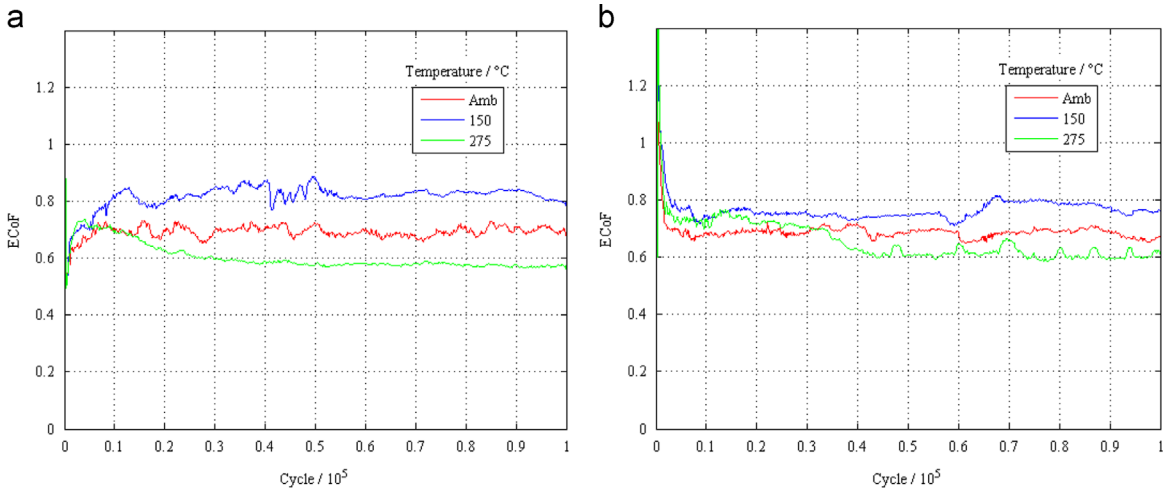

Fig. 10. Energy coefficients of friction with the test frquencies of (a) 20 Hz and (b) 200 Hz.

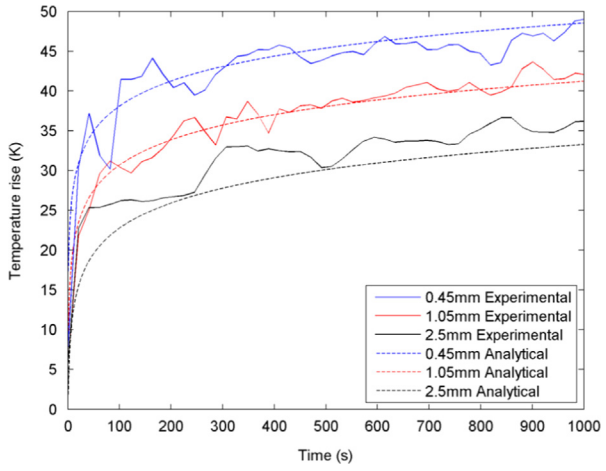

Fig. 11. Comparison of measured temperature rises and analytical results calculated by the mathematical model for different distances from the contact (P=450 N, f=200 Hz, Δ=50 μm, room temperature).

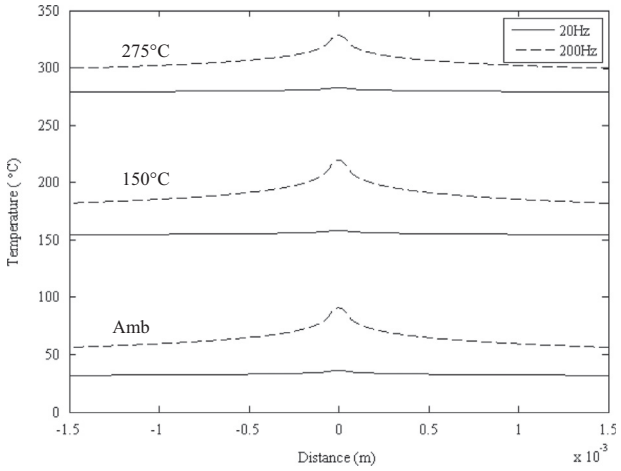

Fig. 12. Prediction of local surface temperatures in contact after 100,000 fretting cycles (P=450 N, Δ=50 μm) as a function of distance from the centre of the contact.

steel. Bulk material removal was observed at room temperature at both fretting frequencies (despite the actual contact temperature at the higher frequency being predicted to reach temperatures of greater than 90 °C – see Fig. 12). Following testing at both frequencies, very little build-up of material was seen outside the worn contact patch, and the scars themselves appeared very similar, with evidence of a good deal of oxide retention within the scar, but also evidence of metallic surface in the scar (indicating that loss of the oxide debris bed was occurring readily throughout the scar). At both frequencies, the coefficient of friction was almost identical, again providing evidence that the frequency had little effect on behaviour at this bulk temperature, despite the differences in predicted temperature in the contact, and differences in the time interval between passes of the contact.

For the tests conducted at the highest temperature (275 °C), narrow wear scars with material build up at both sides were observed following fretting at both frequencies; in both cases, the net wear rate is almost zero, with the wear rate and transfer rate

being well balanced. The BSE-SEM images indicate that in both cases, there is a full coverage of the wear scar by a dense oxide bed. Also, only very small amounts of loose debris were observed when the fretting contacts were disassembled at the ends of the tests at this temperature (following tests at both frequencies). The energy coefficient of friction was also very similar for the tests conducted at the two frequencies. The temperature at the centre of the contact for the test conducted at 200 Hz is predicted to be about 50 °C higher than that of the contact in the test conducted at 20 Hz (itself showing very little increase above the specimen bulk temperature of 275 °C); however, it is clear that this predicted difference in temperature exerts little influence on the development of wear within this system. Many workers have observed that once the temperature in a fretting contact has increased above a certain value, then the net wear volume (and wear behaviour) is not strongly dependent upon further rises in temperature; the critical temperature is that where the temperature is high enough to result in sintering and retention of oxide in the contact in the form of a protective oxide debris bed. It is proposed that at 275 °C, the bulk temperature is high enough to result in the development of a protective oxide debris bed, and that the additional increase in temperature associated with the higher test frequency does not therefore exert a strong influence. It is clear that the reduction in time between passes at the higher test frequency also exerts little influence in the development of wear in this system.

Accordingly, the only significant differences in fretting behaviour with frequency are observed at the intermediate temperature of 150 °C. The tests at 150 °C result in the most extensive damage to the surface, especially at the lower frequency. The rate of formation of the oxide in the contact is promoted by the increase in ambient temperature, but the temperature (at either frequency) is clearly not high enough to result in the full formation of an adherent and stable debris bed in the contact (although the debris retention in the contact appears to be high at any one time, as observed in Figs. 8 and 9). As such, the wear scars are deep. However, the overall wear rate is much lower at this temperature for the test conducted at the higher frequency, and it is proposed that this reduction results from the higher contact temperature at the higher frequency which is able to more successfully promote debris retention in the contact.

6. Conclusions

The effect of temperature on the development of fretting damage in 304 stainless steel (well known in the literature) has been shown to be influenced by the frequency of fretting. There is dissipation of frictional power in the contact, which at elevated frequencies has been shown to have a measurable effect on the contact temperature. A simple analytical model has been developed which indicates that at 200 Hz, the increase in contact temperature due to dissipation of frictional power may be greater than 70 °C.

There is known to be a critical temperature in fretting tests, above which the debris bed is efficiently retained in the contact and forms a protective bed. Under the conditions examined in this programme, the additional frictional power dissipation associated with high frequency fretting was not enough to exceed this critical temperature when the bulk temperature was room temperature. It was also shown that a bulk temperature of 275 °C was already above the critical temperature, and so again, the increase in temperature associated with the frictional power dissipation exerted little influence. However, with a bulk temperature of 150 °C, the frictional power dissipation raised the temperature of the contact fretted at the higher frequency above the critical temperature; accordingly, a strong dependence of fretting behaviour upon fretting frequency was observed at this temperature.

Acknowledgements

The authors wish to thank the Taiho Kogyo Tribology Research Foundation, Toyota City, Japan for supporting an upgrade of the experimental facilities which have underpinned this work. The views expressed in this paper are those of the authors and not necessarily those of the Taiho Kogyo Tribology Research Foundation.

The authors would also like to thank the University of Nottingham for the award of the “Dean of Engineering Research Scholarship for International Excellence” to Xiaozhe Jin.

References

[1] J.M. Dobromirski, Variables of Fretting Process: Are There 50 of Them? Standardization of Fretting Fatigue Test Methods and Equipment, ASTM, Philadelphia (1992) 60–66.
[2] P.L. Hurricks, The fretting wear of mild steel from 200 to 500 °C, Wear 30 (1974) 189–212. http://dx.doi.org/10.1016/0043-1648(74)90175-6.
[3] P.L. Hurricks, The fretting wear of mild steel from room temperature to 200 °C, Wear 19 (1972) 207–229. http://dx.doi.org/10.1016/0043-1648(72)90304-3.
[4] R. Rybiak, S. Fouvry, B. Bonnet, Fretting wear of stainless steels under variable temperature conditions: introduction of a “composite” wear law, Wear 268 (2010) 413–423. http://dx.doi.org/10.1016/j.wear.2009.08.029.
[5] T. Kayaba, A. Iwabuchi, The fretting wear of 0.45% C steel and austenitic stainless steel from 20 to 650 °C in air, Wear 74 (1981) 229–245. http://dx.doi.org/10.1016/0043-1648(81)90165-4.
[6] H.H. Uhlig, Mechanism of fretting corrosion, J. Appl. Mech. ASME 21 (1954) 401–407.
[7] I. Feng, H.H. Uhlig, Fretting corrosion of mild steel in air and in nitrogen, J. Appl. Mech. ASME 21 (1954) 395–400.
[8] A.R. Warmuth, The effect of contact geometry and frequency on dry and lubricated fretting wear, University of Nottingham, UK, 2014, Ph.D. thesis.
[9] C. Colombie, Y. Berthier, A. Floquet, L. Vincent, M. Godet, Fretting: load carrying capacity of wear debris, J. Tribol. Trans. ASME 106 (1984) 194–201. http://dx.doi.org/10.1115/1.3260881.
[10] M. Godet, The third-body approach: a mechanical view of wear, Wear 100 (1984) 437–452. http://dx.doi.org/10.1016/0043-1648(84)90025-5.
[11] J. Jiang, F.H. Stott, M.M. Stack, The role of triboparticulates in dry sliding wear, Tribol. Int. 31 (1998) 245–256. http://dx.doi.org/10.1016/S0301-679X(98)00027-9.
[12] R.M. German, Sintering Theory and Practice, John Wiley & Sons (A WileyInterscience Publication), 1996.
[13] H. Kato, K. Komai, Tribofilm formation and mild wear by tribo-sintering of nanometer-sized oxide particles on rubbing steel surfaces, Wear 262 (2007) 36–41. http://dx.doi.org/10.1016/j.wear.2006.03.046.
[14] H. Kato, Effects of supply of fine oxide particles onto rubbing steel surfaces on severe–mild wear transition and oxide film formation, Tribol. Int. 41 (2008) 735–742. http://dx.doi.org/10.1016/j.triboint.2008.01.001.
[15] K. Adachi, K. Kato, Formation of smooth wear surfaces on alumina ceramics by embedding and tribo-sintering of fine wear particles, Wear 245 (2000) 84–91. http://dx.doi.org/10.1016/S0043-1648(00)00468-3.
[16] S.R. Pearson, P.H. Shipway, J.O. Abere, R.A.A. Hewitt, The effect of temperature on wear and friction of a high strength steel in fretting, Wear 303 (2013) 622–631. http://dx.doi.org/10.1016/j.wear.2013.03.048.
[17] S. Söderberg, U. Bryggman, T. McCullough, Frequency effects in fretting wear, Wear 110 (1986) 19–34. http://dx.doi.org/10.1016/0043-1648(86)90149-3.
[18] L. Toth, The investigation of the steady stage of steel fretting, Wear 20 (1972) 277–286. http://dx.doi.org/10.1016/0043-1648(72)90409-7.
[19] G.H.G. Vaessen, C.P.L. Commissaris, A.W.J. de Gee, Fretting corrosion of Cu–Ni–Al against plain carbon steel, Arch. Proc. Inst. Mech. Eng. Conf. Proc. (1964-1970), http://dx.doi.org/10.1243/PIME_CONF_1968_183_286_02, Var. Titles Label. Vol. A to S. 183 (1968) 125–128.
[20] H. Blok, The dissipation of frictional heat, Appl. Sci. Res., Sect. A 5 (1955).
[21] M.F. Ashby, J. Abulawi, H.S. Kong, Temperature maps for frictional heating in dry sliding, Tribol. Trans. 34 (1991) 577–587. http://dx.doi.org/10.1080/10402009108982074.
[22] J.F. Archard, The temperature of rubbing surfaces, Wear 2 (1959) 438–455. http://dx.doi.org/10.1016/0043-1648(59)90159-0.
[23] M.H. Attia, N.S. D'Silva, Effect of mode of motion and process parameters on the prediction of temperature rise in fretting wear, Wear 106 (1985) 203–224. http://dx.doi.org/10.1016/0043-1648(85)90110-3.
[24] J.A. Greenwood, A.F. Alliston-Greiner, Surface temperatures in a fretting contact, Wear 155 (1992) 269–275. http://dx.doi.org/10.1016/0043-1648(92)90086-N.
[25] J. Wen, M.M. Khonsari, Transient temperature involving oscillatory heat source with application in fretting contact, J. Tribol. 129 (2007) 517. http://dx.doi.org/10.1115/1.2736435.

[26] S. Fouvry, P. Kapsa, H. Zahouani, L. Vincent, Wear analysis in fretting of hard coatings through a dissipated energy concept, Wear 203-204 (1997) 393–403. http://dx.doi.org/10.1016/S0043-1648(96)07436-4.
[27] S.R. Pearson, P.H. Shipway, Is the wear coefficient dependent upon slip amplitude in fretting? Vingsbo and Söderberg revisited, Wear (2014), http://dx.doi.org/10.1016/j.wear.2014.11.005.
[28] K.L. Johnson, Contact Mechanics, Cambridge University Press, Cambridge, 1987.
[29] H.S. Carslaw, J.C. Jaeger, Conduction of heat in solids, Oxford Clarendon Press, London, 1959.
[30] M.W. Chase, NIST-JANAF thermochemical tables, fourth edition, J. Phys. Chem. Ref. Data, Monogr. 9 (1998).
[31] J.D. Lemm, A.R. Warmuth, S.R. Pearson, P.H. Shipway, The influence of surface hardness on the fretting wear of steel pairs—Its role in debris retention in the contact, Tribol. Int. 81 (2015) 258–266. http://dx.doi.org/10.1016/j.triboint.2014.09.003.